High Precision GPS Attitude Determination using the AAU Testbed

STVF

Doc. No.: I-2000-602801

Work Package: 1.0

Prepared by: Mikkel Jensen, Thomas Bak

Approved by:
Status: Issue 1.0
Clasification: Distribution limited
Date: 27/6 2000
File: attitude
Pages: 42

Aalborg University
Department of Control Engineering
Fredrik Bajers Vej 7C
DK-9220 Aalborg Ø
Denmark
Tel.: +45 9635 8761
Fax.: +45 9815 1739
E-mail: tb@control.auc.dk

Document History

Issue:	Date:	Author:	Pages:	Description:
0.1	14-10-99	mj	All	First draft issue
1.0	26-06-00	tb	All	Corrections to draft issue implemented

Acknowledgment

This work was supported by the Danish Research Council (STVF) under contract number 602801. Funding for hardware was provided by Det Obelske Familiefond.

Abstract

A platform for testing attitude determination algorithms based on real-time differential phase measurements of GPS signals has been constructed. The attitude is estimated using a phase interferometry technique on waveforms received by multiple antennas. Angle encoders on the antenna array provide the true attitude. Several different algorithms, recent as well as well-proven, have been implemented and tested. An Extended Kalman filter, including an accurate model of the spacecraft dynamics, achieves an accuracy better than 0.1 deg. (1σ) which is the requirement for high precision missions. The remaining algorithms perform almost identically with an accuracy of 0.25 deg. (1σ) approximately. Simulation tests revealed that the antenna configuration has a profound impact on performance, calling for further investigations into this field.

The relative nature of the encoders cause an offset error to appear on the angle estimate. A problem which is avoided by a prospective upgrade of the platform to include a star tracker.

This report report is divided into six chapters. Chapter 1 addresses the attitude problem and describe the AAU testbed. Chapter 2 defines the coordinate systems used in this report and describes the rotations needed to convert coordinates from one system to another. Chapter 3 introduces the method of interferometry and describes each of the implemented algorithms in detail. The result of accuracy, speed and convergence tests performed using simulated data is presented in chapter 4. Finally, the conclusion to this report can be found in chapter 5 along with a recommendation for future work. Serving as an appendix to this report, chapter 6 discusses the possibility of improving the quality of the results by equipping the existing test platform with a high accuracy reference.starts out by describing the attitude determination problem and possible ways to address this problem, and the AAU GPS testbed is described.

Contents

List of Figures

List of Tables

1 Introduction

Determination of attitude is an important part of any space mission. Knowledge of the attitude is required for optimal pointing of antennas and solar panels to ensure communication and power to the spacecraft. Furthermore, if the spacecraft is carrying scientific instruments, these often need to be pointed with high accuracy. Without a precise attitude reference the scientific mission may degrade.

Current methods of attitude determination includes one or more of the following sensors

- Gyroscopes
- Star sensors
- Sun sensors
- Earth horizon sensors
- Magnetometers

Rate gyros measures the angular velocity around a given axis with respect to an inertial reference frame. They are often combined with the other vector based sensors to provide information of state and to increase the bandwidth of the system. Due to drift in bias the attitude error resulting from integration of the sensor output will grow without bounds. Hence, regular attitude fixes from other sensors are needed to provide information of bias and to limit the error.

Star, sun and horizon sensors all measure the direction of a known vector in a coordinate frame fixed to the body of the spacecraft. Combining these vector measurements with their known references in the inertial frames, n vector pairs are obtained. The searched attitude is then obtained using vector matching techniques. Magnetometers measure the strength as well as the direction of the local field. A model of the Earths magnetic field is used as reference.

Sensor	Performance
Rate gyros	drift: 0.002 deg/hr - 1 deg/hr
Star sensors	1 arc sec - 1 arc min
Sun sensors	0.005 deg - 4 deg
Horizon sensors	0.05 - 1 deg
Magnetometers	0.5 deg - 1 deg

Table 1.1: Accuracy of commonly used sensors [Bak, 1999]

The star sensor is generally the most accurate of the types mentioned but due to optical smearing it can only be applied for limited angular rates. Sun sensors require a clear line-of-sight to the sun, and attitude information is hence lost during the eclipse part of the orbit. Magnetometers are highly sensitive to local magnetic fields generated by onboard electronics. Their precision is limited by the uncertainty of the reference field making them most suitable for low earth orbits where the field is strong and well known.

The Global Positioning System presents a new and accurate way of determining the attitude. The method is based on the carrier wave rather than the encoded data as used for positioning

purposes. The working principle is known as carrier phase interferometry and explained in detail in section 3.1.

GPS is currently used on board spacecraft for timing and orbit determination only. Adding the capability of attitude determination requires little more than some extra antennas and phase sampling circuitry, making this solution light and inexpensive.

One of the first successful experiments of GPS attitude determination was implemented on the radar calibration satellite RADCAL [Lightsey et al., 94]. The results showed an estimation error of 0.5 - 1.0 deg RMS for relatively small baselines (< 1m), proving this technology usable for coarse accuracy missions.
The GPS system has by now passed the experimental stage, and it is planned that the International Space Station, which is currently under construction, will use GPS as its primary method of attitude determination [Shaki, 1998].

1.1 The AAU Testbed

The purpose of this report is to implement and test some of the more recent and promising algorithms based on data gathered from a custom-built test platform. The accuracy aimed at is 0.1 deg RMS or better, enabling the GPS system to serve as backup sensor on high-accuracy missions, or as main sensor on missions with lower requirements.

The test platform is shown in figure 1.1.

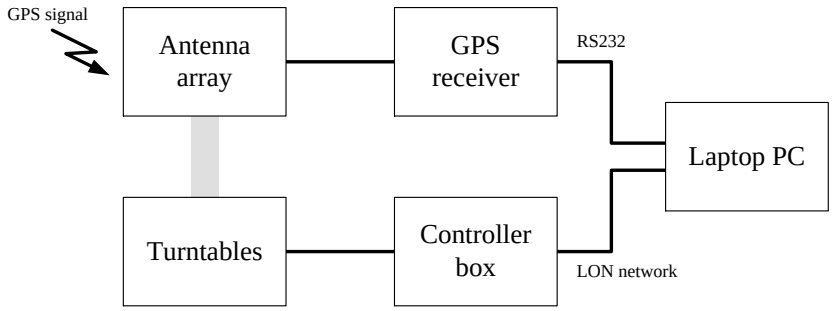

Figure 1.1: The AAU testbed. Mechanical connections shown by grey bars and electrical connections are shown by black lines.

Antenna array

The antenna array consists of four *Trimble* antennas mounted in a square formation with diagonal length of 1 meter. All antennas are lying in the same plane and their formation defines the body coordinate frame as shown in figure 2.1. Below each antenna is mounted a circular aluminum plate which protects the antenna from ground reflections. This reduces the multipath by screening off signals from below the antenna plane. The four arms holding the antennas are made from aluminum tubes ensuring a very rigid construction. The antennas have a well defined phase-center and consist of a flat micro strip element and a preamplifier circuit built into a single unit.

GPS receiver

The *Trimble TANS Vector* GPS receiver is the heart of the operation. The TANS Vector is a four-antenna attitude determination system which measures the three-axis orientation (azimuth, pitch and roll) of an object, as well as its three-dimensional position, velocity, and time. Military operations use the TANS Vector to guide autonomous aircraft used for reconnaissance missions and mine detection. The system includes a Receiver Processor Unit (RPU) with a bi-directional RS-422 interface and four GPS antenna.

It has the task of sampling the phase differences of the electric signals from the antennas, and communicate these through a serial RS-422 connection together with the position of the satellites, obtained from the ephemeris data. The receiver also provides its own attitude determination as well as standard or differential GPS position, velocity and time data. The specified accuracy of the attitude estimate is 0.3 deg RMS for 1m baselines, and 0.07 deg RMS for baselines of 4m, which is the maximum recommended length. The integer part of the phase difference is calculated using an integer search algorithm, and included in the data packets. The maximum speed at which the receiver can compute attitude solutions is 10 Hz. Line-of-sight vectors are, however, computed asynchronously since these are obtained from the ephemeris data which is only transmitted approximately every 30 seconds by the GPS satellite.

Rotation Stages

The antenna array is mounted on three orthogonal *Newport* rotation stages allowing three degrees of freedom. The turntables are mounted on top of each other causing the combined rotation to be described as an Euler sequence. If the body and reference coordinate systems are defined as in section 2.1 and 2.3 respectively, then the rotation between these two systems is given by a 2-1-3 Euler sequence of the table angles.

$$\mathbf{A}_{213} = \begin{bmatrix} \cos\psi\cos\phi + \sin\psi\sin\theta\sin\phi & \sin\psi\cos\theta & -\cos\psi\sin\phi + \sin\psi\sin\theta\cos\phi \\ -\sin\psi\cos\phi + \cos\psi\sin\theta\sin\phi & \cos\psi\cos\theta & \sin\psi\sin\phi + \cos\psi\sin\theta\cos\phi \\ \cos\theta\sin\phi & -\sin\theta & \cos\theta\cos\phi \end{bmatrix} \quad (1.1)$$

The angles at which the lower two turntables can be rotated is mechanically limited to $\pm$ 15 degrees. Due to cable windup the upper turntable is unable to rotate more than 720 degrees. Furthermore, since the turntables were build for precision rather than speed, the maximum angular velocity is about 1.5 deg/sec around all three axes. Encoders built into the turntables measure the angle at which the table is rotated with a resolution of 0.002 degrees. The encoders, however, only measure angles relative to the initial position creating the need for manual alignment before the angles are reset. If the turntables are operated beyond their maximum speed capability garbled data will be read of the encoders.

Controller box

The purpose of the controller box is to control the angles of the turntables. The box contains three Local Operating Network (*LON*) units from Echelon each controlling a separate turntable. Each unit implements a fully configurable PID regulator which can be operated in either position or speed mode. Set-points for the regulators are transmitted over the LON network and the encoders can be polled using commands issued over the network.

The accuracy at which the tables can be aligned equals the encoder resolution of 0.002 degrees,

required that the tables are allowed to settle. Settling time depends on regulator parameters, operation mode and the step size in the set-point. Using the default regulator parameters and a step size of about one degree in position mode at least one second should be allowed in settling time.

Laptop PC

A laptop PC controls the execution of the experiment. Interfaces are provided for serial connection (RS422) as well as a PCMCIA interface to the LON network. The main tasks of the PC can be split into four tasks.

- Initialization and configuration of GPS receiver and LON network
- Set attitude of antenna array according to turntable angles from file
- Store the actual obtained angles on file.
- Store time, phase and line-of-sight data from GPS receiver on file

Initialization and configuration is performed only once at startup, while the three remaining tasks are repeated at each sample time. To ensure agreement between the measurements each of the three tasks are implemented as a real-time task under a DOS kernel. A time trigger pulse from the GPS receiver is used to synchronize the tasks. All data is recorded to file for offline processing sampled at a rate of 1 Hz.

1.2 Outline of the report

The remainder of this report is divided into five chapters. Chapter 2 defines the coordinate systems used in this report and describes the rotations needed to convert coordinates from one system to another. Chapter 3 introduces the method of interferometry and describes each of the implemented algorithms in detail. The result of accuracy, speed and convergence tests performed using simulated data is presented in chapter 4. Finally, the conclusion to this report can be found in chapter 5 along with a recommendation for future work. Serving as an appendix to this report, chapter 6 discusses the possibility of improving the quality of the results by equipping the existing test platform with a high accuracy reference.

2 Coordinate systems

The attitude of a spacecraft can be expressed as the rotation of a body coordinate systems with respect to a reference frame. The body coordinate system is fixed to the body of the spacecraft while the reference frame often is chosen as the local horizontal, or alternatively, an inertial coordinate system.

2.1 The body coordinate system

The body coordinate system (uvw) is often used to define the position and direction of instruments carried by the spacecraft.

It is defined with respect to the antenna array as shown in figure 2.1. The antenna array consists

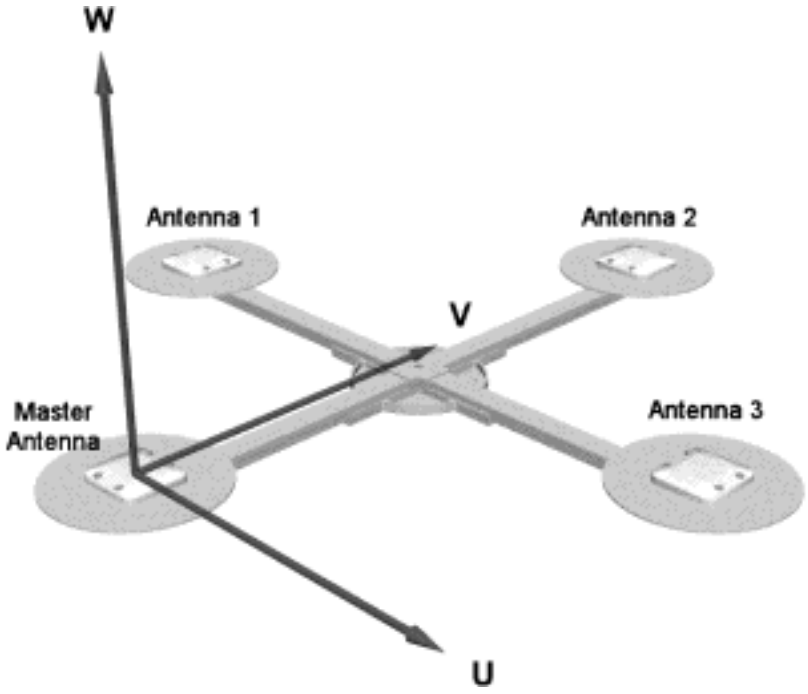

Figure 2.1: The body coordinate system.

of four antennas. The antennas are positioned in each corner of a square with a diagonal length of one meter. The four antennas are designated as Master, 1, 2 and 3.

The direct line from the Master antenna to one of the other antennas is called a baseline. The body system is defined by the three baselines. The origin of this system is defined by the master antenna.

- The W-axis points in a direction perpendicular to the plane defined by antenna 1, 3 and the Master antenna (M13).
- The V-axis is defined as the projection of baseline 2 onto the M13 plane.
- The U-axis completes a right handed orthogonal system ($\mathbf{u} \times \mathbf{v} = \mathbf{w}$).

The baselines can be described by the vectors

$$\mathbf{b}_1 = \begin{bmatrix} -0.5 \\ 0.5 \\ 0 \end{bmatrix} \qquad \mathbf{b}_2 = \begin{bmatrix} 0 \\ 1 \\ 0 \end{bmatrix} \qquad \mathbf{b}_3 = \begin{bmatrix} 0.5 \\ 0.5 \\ 0 \end{bmatrix} \tag{2.1}$$

2.2 ECEF coordinate system

The *Earth Centered, Earth Fixed* coordinate system is often used to define three dimensional position with respect to the Earth's center of mass.

- The Z-axis points toward the North Pole.
- The X-axis is defined by the intersection of the plane defined by the prime meridian and the equatorial plane.
- The Y-axis completes a right handed orthogonal system ($\mathbf{x} \times \mathbf{y} = \mathbf{z}$).

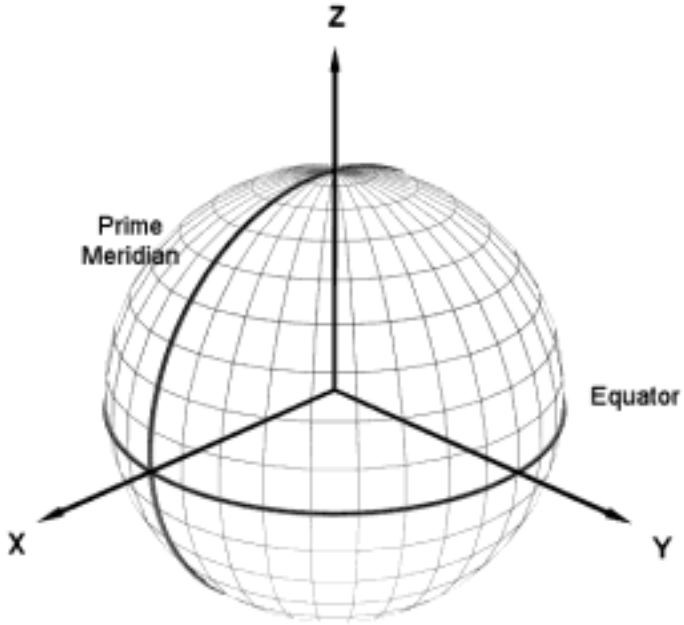

Figure 2.2: The ECEF coordinate system.

Reference ellipsoid
The reference ellipsoid for the World Geodetic System of 1984 (WGS-84) is defined by:

- Equatorial radius (Semi-major axis) $a = 6378137.0$ m
- Flattening $f = 1/298.257223563$

which means that

- Polar radius (Semi-minor axis) $b = a\,(1-f) = 6356752.3142$ m
- Eccentricity squared $e^2 = 2f - f^2 = 0.00669437999013$

This ellipsoidal model can represent the shape of the Earth over the smoothed, averaged sea-surface to within about one-hundred meters. To improve on this accuracy a geoid height model can be used to extend the reference ellipsoid. Geoid models attempt to represent the surface of the entire Earth over both land and ocean as though the surface resulted from gravity alone. Local variations in gravity, caused by variations in the earth's core and surface materials, cause this gravity surface to be irregular.

The U. S. National Imagery and Mapping Agency has published a ten by ten degree grid of geoid heights for the WGS-84 geoid.

By using a four point linear interpolation algorithm at the four closest grid points, the geoid height for any location can be determined. With this correction the accuracy is about one meter. This is refered to as the *mean sea level* (MSL) or in other words, the sea level when no tidal forces are present.

Coordinate conversion from LLA to ECEF
Due to the ellipsoidal shape of the Earth, angular coordinates such as *longitude*, *latitude* and *altitude* (LLA) must be converted to cartesian ECEF coordinates in the following manner.

$$X = (N+h)\cos\phi\,\cos\lambda \tag{2.2}$$
$$Y = (N+h)\cos\phi\,\sin\lambda \tag{2.3}$$
$$Z = [N(1-e^2)+h]\sin\phi \tag{2.4}$$

where ϕ is the latitude, λ is the longitude and h is the height above the ellipsoid (HAE).

The radius of curvature, N, in the prime vertical can be expressed as

$$N = \frac{a}{\sqrt{1-e^2\sin^2\phi}} \tag{2.5}$$

2.3 ENU coordinate system

The *East*, *North* and *Up* axes of the ENU-system comprises a local horizontal coordinate system on a specific point on the WGS-84 ellipsoid. This system is used for defining coordinates relative to a fixed position on the surface of the earth. It is the reference system for attitude

- The North-axis points toward true North.
- The Up-axis points away from the earth in a direction perpendicular to the local horizontal plane.
- The East-axis completes a right handed orthogonal system $(East \times North = Up)$ pointing toward true East.

Rotation from ECEF to ENU
The rotation from ECEF to ENU can be described as two consecutive rotations about the coordinate axes, followed by a shift in the axes.

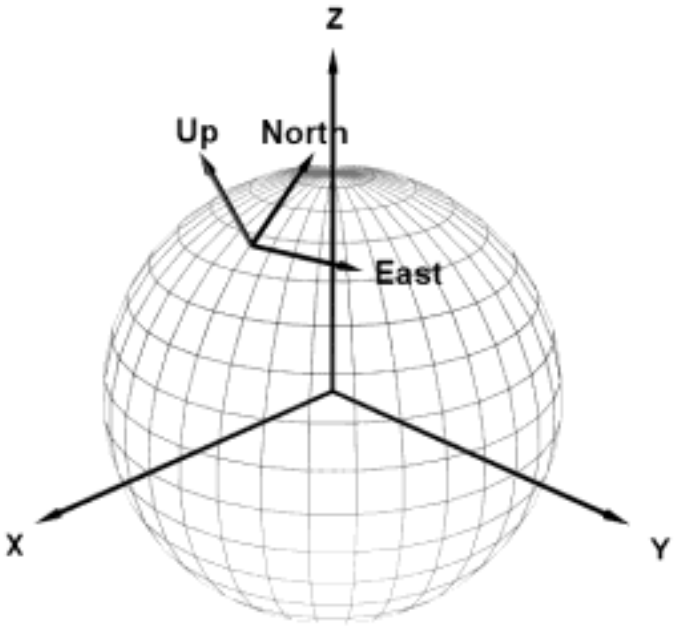

Figure 2.3: The ENU coordinate system.

The first rotation, $\mathbf{A}_3(\lambda)$, is about the third axis of the ECEF system by an angle of λ, where λ is the longitude of the position. This is followed by a rotation, $\mathbf{A}_2(-\phi)$, in the negative direction about the second axis of the new coordinate system. The angle of this rotation is given by ϕ, which is the northern latitude of the position. Finally, the axes are shifted by the rotation $\mathbf{A}_{shift}$ such that *East*, *North* and *Up* refers to the first second and third axes, respectively.

$$\mathbf{A}_{shift} = \begin{bmatrix} 0 & 1 & 0 \\ 0 & 0 & 1 \\ 1 & 0 & 0 \end{bmatrix} \tag{2.6}$$

$$\mathbf{A}_{ECEF}^{ENU} = \mathbf{A}_{shift}\mathbf{A}_2(-\phi)\mathbf{A}_3(\lambda) = \begin{bmatrix} -\sin\lambda & \cos\lambda & 0 \\ -\sin\phi\cos\lambda & -\sin\phi\sin\lambda & \cos\phi \\ \cos\phi\cos\lambda & \cos\phi\sin\lambda & \sin\phi \end{bmatrix} \tag{2.7}$$

3 Algorithms

Symbol	Size	Description
$\boldsymbol{\beta}$	$\mathcal{R}^{3\times 1}$	line bias vector
$\boldsymbol{\omega}$	$\mathcal{R}^{3\times 1}$	angular velocity vector
$\boldsymbol{\Omega}$	$\mathcal{R}^{4\times 4}$	skew-symmetric matrix of $\boldsymbol{\omega}$
ϕ	$\mathcal{R}$	fractional part of phase offset
$\mathbf{A}$	$\mathcal{R}^{3\times 3}$	rotation matrix
$\mathbf{b}$	$\mathcal{R}^{3\times 1}$	baseline vector
$\mathbf{B}$	$\mathcal{R}^{3\times m}$	matrix of baselines
$\mathbf{f}$	$\mathcal{R}^{l\times 1}$	model vector
$\mathbf{F}$	$\mathcal{R}^{(l-1)\times(l-1)}$	model gradient matrix
$\mathbf{h}$	$\mathcal{R}^{mn\times 1}$	measurement estimate vector
$\mathbf{H}$	$\mathcal{R}^{mn\times(l-1)}$	measurement gradient matrix
k	$\mathcal{Z}$	number of wavelengths in phase offset
$\mathbf{K}$	$\mathcal{R}^{(l-1)\times mn}$	Kalman gain matrix
l	$\mathcal{N}$	number of elements in state vector
m	$\mathcal{N}$	number of baselines
n	$\mathcal{N}$	number of satellites
$\mathbf{P}$	$\mathcal{R}^{(l-1)\times(l-1)}$	prediction error covariance matrix
$\boldsymbol{q}$	$\mathcal{R}^{4\times 1}$	attitude quaternion
$\mathbf{q}$	$\mathcal{R}^{3\times 1}$	three component quaternion
$\mathbf{Q}$	$\mathcal{R}^{(l-1)\times(l-1)}$	model noise covariance matrix
Δr	$\mathcal{R}$	phase offset including integer part
$\Delta\mathbf{R}$	$\mathcal{R}^{m\times n}$	matrix of phase offsets
$\mathbf{R}$	$\mathcal{R}^{mn\times mn}$	measurement noise covariance matrix
$\mathbf{s}$	$\mathcal{R}^{3\times 1}$	line-of-sight vector
$\mathbf{S}$	$\mathcal{R}^{3\times n}$	matrix of line-of-sight vectors
v	$\mathcal{R}$	zero-mean Guassian white noise
w	$\mathcal{R}$	weight assigned to each measurement
$\mathbf{x}$	$\mathcal{R}^{l\times 1}$	state vector
$\mathbf{W}_B$	$\mathcal{R}^{m\times m}$	matrix of weight factors
$\mathbf{W}_S$	$\mathcal{R}^{n\times n}$	matrix of weight factors
$\mathbf{z}$	$\mathcal{R}^{mn\times 1}$	measurement vector

Table 3.1: List of symbols (Time and sequence indexing removed)

3.1 Principle of interferometry

The basic principle of attitude determination using GPS signals is shown in figure 3.1.

A signal transmitted from a distant GPS satellite arrives at the closest antenna slightly before reaching the other. By measuring the difference in carrier phase between the two antennas, a receiver can determine the relative distance Δr between the antennas in the direction of the GPS satellite.

The direction towards the GPS satellite is denoted by the line-of-sight vector $\mathbf{s}$ of unit length, and the baseline between the Master and the Slave antenna is denoted by the vector $\mathbf{b}$ given in

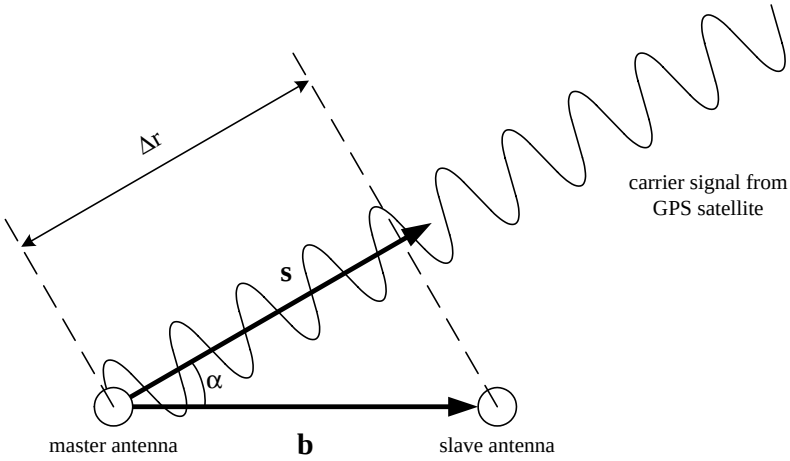

Figure 3.1: Carrier phase interferometry.

wavelengths. In this case we can define the relative distance as the projection of the baseline vector onto the line-of-sight vector.

$$\Delta r = |\mathbf{b}| \cos \alpha = \mathbf{b}^T \mathbf{s} \tag{3.1}$$

If the length of the baseline is longer than one wavelength, which is most often the case, the relative distance Δr may contain some integer-part value k which cannot be measured directly.

$$\Delta r = \phi + k \tag{3.2}$$

The integer k must be determined from the actual measured fractional part ϕ of the differential phase. This is done in an *integer search algorithm* which has to be performed at startup before any attitude determination can take place, see [Conway et al., 1996] and [Crassidis et al., 1999b]).

Once the integer part has been found a simple algorithm keeps track of any integer wrap-arounds in the ϕ measurements. Thus the only ambiguity is the initial value of the integer k which need to be solved for only once. Here we will assume that the integer part has already been found and included in the phase measurements, effectively making Δr the measured quantity.

The components of the line-of-sight vector $\mathbf{s}$ is known in some reference frame like *ECI* or *ENU* and the baseline vector $\mathbf{b}$ is given in the body frame (see sections 2.1 and 2.3 for definitions). If the attitude of the body frame with respect to the reference frame is described by rotation matrix $\mathbf{A}$, then the differential phase measurement is given by

$$\Delta r = (\mathbf{b}^B)^T \mathbf{A}_R^B \mathbf{s}^R + \beta + v \tag{3.3}$$

where β is the linebias and v is the measurement noise.

The B and R denotes the body frame and reference frame respectively. In the following this notation will be dropped and baselines is implicitly defined in the body frame and the line-of-sight vectors in the reference frame, unless otherwise stated.

Linebias is caused by the uneven time delays when the electric signals travel from the antenna to the receiver. By making the antenna cables equal in length this disturbance is minimized. This

time delay varies with the temperature but due to the differential nature of the receiver the offset is effectively constant over a certain temperature range. Still, this bias must be removed before estimating the attitude.

An optimal attitude solution for a given set of range measurements, Δr_{ij}, taken at a single epoch for baseline i and satellite j is obtained by minimizing the quadratic cost function

$$J(\mathbf{A}) = \sum_{i=1}^{m}\sum_{j=1}^{n} w_{ij}(\Delta r_{ij} - \mathbf{b}_i^T \mathbf{A}\mathbf{s}_j)^2 \tag{3.4}$$

where m is the number of baselines, n is the number of satellites and w_{ij} is a weight assigned to each range measurement. In equation (3.4) it is assumed that the range measurements have been corrected for linebias and integer parts.

The value of the weights w_{ij} should be an indication of the uncertainty in the measurements. If the measurement noise v is zero-mean Gaussian white noise with covariance σ_{ij}^2, then the maximum likelihood estimate for w_{ij} is given by σ_{ij}^{-2}.

Closely related to this cost function is *Wahba's problem*. The problem was posed in 1965 by Grace Wahba as finding the optimal attitude matrix $\mathbf{A}$ that minimizes the cost function

$$J(\mathbf{A}) = \sum_{j=1}^{n} w_j(\mathbf{s}_j^B - \mathbf{A}\mathbf{s}_j^R)^2 \tag{3.5}$$

where $\mathbf{s}_j^B$ is the jth measured line-of-sight vector in the body frame, $\mathbf{s}_j^R$ is the known line-of-sight vector in the reference frame, and w_j is an optional weighting factor.

Attitude determination using vector observations originates from early work on spacecrafts equipped with celestial sensors. The line-of-sight vectors of a large number of stars is known with great accuracy in the inertial frame. By correlating these with body-referenced vector measurements obtained from a star tracker, the optimal attitude can be found by minimizing equation (3.5) with respect to $\mathbf{A}$.

Many efficient algorithms exist for solving Wahba's problem. In order for these to be applicable to attitude determination using GPS it is necessary to either convert the differential phase measurements into vector observations, or transform the cost function of equation (3.4) to the more general case of (3.5). Still, other algorithms exist which are specific to GPS attitude determination.

In the following some of the more recent algorithms are described, and the strength and weakness of each algorithm is discussed. Figure 3.2 presents an overview of the algorithms.

The problem of estimating the attitude from differential phase measurements can be seen as a process of converting raw measurements into attitude estimates. The task of integer resolution is the initial step in the process, which is followed by line bias calibration. The forming of vector observations can be seen as an intermediate step in the process even though this method is only implemented in a subset of algorithms.

Figure 3.2 also separates the algorithms into iterative and non-iterative. Non-iterative algorithms are generally preferred over gradient based methods for the reason that they are numerically more stable and often faster to compute.

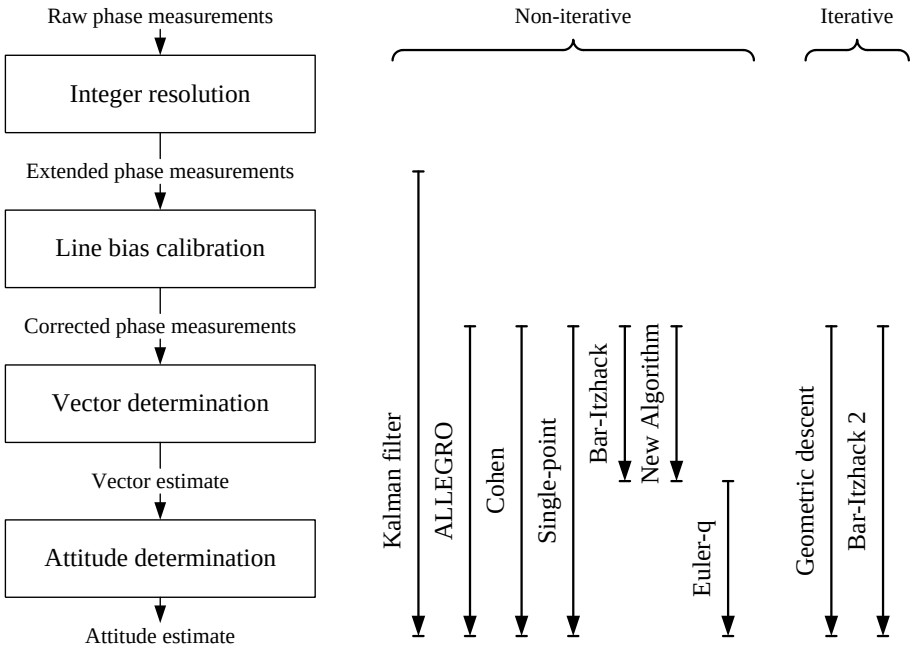

Figure 3.2: The different algorithms

3.2 Extended Kalman filter

The Kalman filter distinguishes itself from the rest of the algorithms in this section due to the fact that it uses a model of the spacecraft movement to help in prediction of the attitude.

Inclusion of the model equations greatly increases the accuracy of this filter, but so does the computations required for each cycle.

At each sample time two quantities are propagated. One is the state, i.e. the attitude and line bias estimates. The second is the state covariance, a measure of the uncertainty in the estimates.

If care is not taken in designing the filter, the update of the state covariance could suffer from numerical round-off errors causing measurement rejection and eventually system instability.

Furthermore, values for the noise covariance matrices $\mathbf{Q}$ and $\mathbf{R}$ must be found in a tuning process prior to filter employment. The filter must be tuned correctly in order to provide (sub)optimal attitude estimates.

The Kalman filter is often based on quaternions to represent the attitude. Quaternions awoid singularities and to minimize the number of computations.

Thus, the state vector contains the attitude quaternion $\boldsymbol{q}$, the angular rate vector $\boldsymbol{\omega}$ and an estimate of the line bias $\boldsymbol{\beta}$.

$$\mathbf{x}(t_k) = \begin{bmatrix} \boldsymbol{q} \\ \boldsymbol{\omega} \\ \boldsymbol{\beta} \end{bmatrix} \tag{3.6}$$

When using quaternions to represent attitude, the update of the state estimate must be performed

according to quaternion algebra. This means

$$\begin{bmatrix} \boldsymbol{q}(t_k^+) \\ \boldsymbol{\omega}(t_k^+) \\ \boldsymbol{\beta}(t_k^+) \end{bmatrix} = \begin{bmatrix} \delta\boldsymbol{q} \otimes \boldsymbol{q}(t_k^-) \\ \delta\boldsymbol{\omega} + \boldsymbol{\omega}(t_k^-) \\ \delta\boldsymbol{\beta} + \boldsymbol{\beta}(t_k^-) \end{bmatrix} \tag{3.7}$$

where $\otimes$ represents quaternion multiplication and the superscripts "-" and "+" denotes the estimate values before and after the measurement update (at time t_k), respectively.

The correction, $\delta\mathbf{x}$, to the state vector is calculated as a function of the actual phase measurements, $\mathbf{z}$, and the estimated phase measurements, $\mathbf{h}$.

$$h_{ij} = (\mathbf{b}_i^B)^T(\mathbf{A}\mathbf{s}_j^R) + \beta_i \tag{3.8}$$

The measurement gradient matrix $\mathbf{H}$ is obtained by linearizing $\mathbf{h}$ around the most recent attitude estimate. Thus, when observing baseline 1, row ij of the gradient matrix is given by

$$H_{ij} = \big[\, -2(\mathbf{A}\mathbf{s}_j^R)^T[\mathbf{b}_i^\times] \big| 0\ \ 0\ \ 0 \big| 1\ \ 0\ \ 0 \big] \tag{3.9}$$

where $[\mathbf{b}_i^\times]$ is the skew-symmetric matrix of $\mathbf{b}_i$.

Between measurement updates the state vector is propagated by numerical integration of the model vector $\mathbf{f}$.

$$\mathbf{f}[\,\mathbf{x}(t_k), t\,] = \begin{bmatrix} \frac{1}{2}\bar{\boldsymbol{\omega}} \otimes \boldsymbol{q} \\ \mathbf{I}^{-1}(-\boldsymbol{\omega} \times \mathbf{I}\boldsymbol{\omega}) \\ \mathbf{0}_{3\times 1} \end{bmatrix} \tag{3.10}$$

where $\bar{\boldsymbol{\omega}}$ is the fourth dimensional equivalent of $\boldsymbol{\omega}$ understood in the sense $\bar{\boldsymbol{\omega}} = [\boldsymbol{\omega}^T\ 0]^T$
$\mathbf{I}$ is the moment of inertia of the spacecraft and the line bias is modelled as a constant.

The model vector consists of a kinematic and a dynamic model of the spacecrafts rotational movement. The model gradient matrix $\mathbf{F}$ is obtained as the derivative of $\mathbf{f}$ with respect to $\mathbf{x}$.

$$\mathbf{F}[\,\mathbf{x}(t_k), t\,] = \begin{bmatrix} -[\boldsymbol{\omega}^\times] & \frac{1}{2}\mathbf{1}_{3\times 3} & \mathbf{0}_{3\times 3} \\ \mathbf{0}_{3\times 3} & \mathbf{I}^{-1}(\,[\mathbf{I}\boldsymbol{\omega}^\times] - [\boldsymbol{\omega}^\times]\mathbf{I}\,) & \mathbf{0}_{3\times 3} \\ \mathbf{0}_{3\times 3} & \mathbf{0}_{3\times 3} & \mathbf{0}_{3\times 3} \end{bmatrix} \tag{3.11}$$

3.3 Single-point

The Single-point algorithm uses a least-squares approximation technique to find the correction to an a-priori estimate of the attitude.

By linearizing equation (3.3) it can be shown that a perturbation in the attitude $\delta\mathbf{q}$ relates to an offset δr in the differential phase measurement Δr in the following way

$$\delta r_{ij} = -2(\mathbf{A}\mathbf{s}_j^R)^T[\mathbf{b}_i^\times]\delta\mathbf{q} \tag{3.12}$$

where $-2(\mathbf{A}\mathbf{s}_j^R)^T[\mathbf{b}_i^\times]$ is the measurement gradient.

The state vector consists of the attitude correction, $\mathbf{x} = \delta\mathbf{q}$, and the phase residual is formed as the difference between the measured and estimated differential phase. An optimal estimate of

the correction can be obtained by stacking the phase residuals and measurement gradients into separate matrices and solving for $\mathbf{x}$ in a least-squares sense.

$$\begin{aligned} \mathbf{Hx} &= \mathbf{z} \Rightarrow \\ \mathbf{x} &= (\mathbf{H}^T\mathbf{H})^{-1}\mathbf{H}^T\mathbf{z} \end{aligned} \tag{3.13}$$

where

$$\mathbf{z} = \begin{bmatrix} \vdots \\ \delta r_{ij} \\ \vdots \end{bmatrix}, \qquad \mathbf{H} = \begin{bmatrix} \vdots \\ -2(\mathbf{A}\mathbf{s}_j^R)^T[\mathbf{b}_i^\times] \\ \vdots \end{bmatrix} \tag{3.14}$$

The full correction quaternion is obtained by forcing the fourth component to 1 and then normalizing to ensure a length of 1.

$$\delta\boldsymbol{q} = norm\left(\begin{bmatrix} \delta q_1 \\ \delta q_2 \\ \delta q_3 \\ 1 \end{bmatrix}\right) \tag{3.15}$$

This is done to keep the small angle assumption made in the linearization of (3.3) that $q_1 \ldots q_3 \approx 0$ and $q_4 \approx 1$.

If the fourth component is calculated directly from the three other $q_4 = \sqrt{1 - q_1^2 - q_2^2 - q_3^2}$, then for large values of $q_1 \ldots q_3$ the fourth component becomes imaginary and the algorithm fails. By use of equation (3.15) the robustness is increased but at the expense of tracking ability.

Finally the a-priori attitude estimate $\boldsymbol{q}'$ is corrected using standard quaternion multiplication

$$\boldsymbol{q} = \delta\boldsymbol{q} \otimes \boldsymbol{q}' \tag{3.16}$$

where $\boldsymbol{q}$ is the estimate using the most recent measurements.

The single-point method is a very simple algorithm. It is not very robust, which will be shown later, and it fails if the a-priori attitude estimate lies far from the correct attitude.

It is however easy to implement but the required calculations grow rapidly with a growing number of satellites. This is due to the matrix inversion of equation (3.13) which can be avoided using a pseudo-inversion technique.

3.4 Cohen

Cohen's method ([Cohen, 1992]) involves a transformation of the cost function in equation (3.4) to the more general case of (3.5) by proper choice of the weight factors.

Once converted to the form identical with Wahba's problem, the optimal $\mathbf{A}$ is obtained by use of Markley's SVD method or Shuster's QUEST algorithm.

The baselines and line-of-sight vectors for a given epoch are concatenated into the matrices $\mathbf{B}$ and $\mathbf{S}$

$$\mathbf{B} = \begin{bmatrix} \mathbf{b}_1 & \mathbf{b}_2 & \ldots & \mathbf{b}_m \end{bmatrix} \qquad \mathbf{S} = \begin{bmatrix} \mathbf{s}_1 & \mathbf{s}_2 & \ldots & \mathbf{s}_n \end{bmatrix} \tag{3.17}$$

and the differential phase measurements are assembled into the matrix $\mathbf{R}$

$$\Delta\mathbf{R} = \begin{bmatrix} \Delta r_{11} & \Delta r_{12} & \dots & \Delta r_{1n} \\ \Delta r_{21} & \ddots & & \vdots \\ \vdots & & \ddots & \vdots \\ \Delta r_{m1} & \dots & \dots & \Delta r_{mn} \end{bmatrix} \tag{3.18}$$

The cost function in equation (3.4) can be converted to the matrix form

$$J(\mathbf{A}) = \left\| \mathbf{W}_B^{\frac{1}{2}} (\Delta\mathbf{R} - \mathbf{B}^T\mathbf{A}\mathbf{S}) \mathbf{W}_S^{\frac{1}{2}} \right\|_F^2 \tag{3.19}$$

where F denotes the Frobenius norm and $\mathbf{W}_B$ and $\mathbf{W}_S$ are weight matrices applicable to the baselines and line-of-sight vectors, respectively.

The Frobenius norm of a matrix $\mathbf{M}$ is defined as

$$\left\|\mathbf{M}\right\|_F^2 = \sum_{i,j} \left|m_{ij}\right|^2 = tr(\mathbf{M}^T\mathbf{M}) \tag{3.20}$$

Hence, equation (3.19) can be expanded to

$$\begin{aligned} J(\mathbf{A}) \quad = \quad & tr(\mathbf{W}_S^{\frac{1}{2}} \Delta\mathbf{R}^T \mathbf{W}_B \Delta\mathbf{R} \mathbf{W}_S^{\frac{1}{2}}) \\ & + tr(\mathbf{W}_S^{\frac{1}{2}} \mathbf{S}^T \mathbf{A}^T \mathbf{B} \mathbf{W}_B \mathbf{B}^T \mathbf{A} \mathbf{S} \mathbf{W}_S^{\frac{1}{2}}) \\ & - 2\, tr(\mathbf{W}_S^{\frac{1}{2}} \Delta\mathbf{R}^T \mathbf{W}_B \mathbf{B}^T \mathbf{A} \mathbf{S} \mathbf{W}_S^{\frac{1}{2}}) \end{aligned} \tag{3.21}$$

By choosing a specific value for $\mathbf{W}_B$ the first two terms become independent of attitude and can be disregarded.

The value of $\mathbf{W}_B$ can be obtained by performing a Singular Value Decomposition of $\mathbf{B}$ such that

$$\mathbf{B} = \mathbf{U}_B \mathbf{\Sigma}_B \mathbf{V}_B^T \tag{3.22}$$

where $\mathbf{U}_B$ and $\mathbf{V}_B$ are unitary matrices and $\mathbf{\Sigma}_B$ is a diagonal matrix of the same dimension as $\mathbf{B}$ and with non-negative diagonal elements in decreasing order.
The value of $\mathbf{W}_B$ is then given by

$$\mathbf{W}_B = \mathbf{V}_B \mathbf{\Sigma}_B^{-2} \mathbf{V}_B^T \tag{3.23}$$

The new cost function which now has to be *maximized* can be expressed as

$$J'(\mathbf{A}) = tr(\mathbf{A}\mathbf{S}\mathbf{W}_S \Delta\mathbf{R}^T \mathbf{W}_B \mathbf{B}^T) = tr(\mathbf{A}\mathbf{C}^T) \tag{3.24}$$

where $\mathbf{C} = \mathbf{B}\mathbf{W}_B \Delta\mathbf{R}\mathbf{W}_S\mathbf{S}^T$.
This is the same cost function that is used to solve Wahba's problem.

The optimal $\mathbf{A}$ can now be obtained by using Markley's SVD method. That is, performing the SVD of the matrix $\mathbf{C}$

$$\mathbf{C} = \mathbf{U}_C \mathbf{\Sigma}_C \mathbf{V}_C^T \tag{3.25}$$

To ensure that the attitude matrix comes out to be proper (right-handed, det=1) the signs of the third column of both unitary matrices $\mathbf{U}_C$ and $\mathbf{V}_C$ are adjusted to yield the proper matrices $\mathbf{U}_+$ and $\mathbf{V}_+$.

$$\mathbf{U}_+ = \mathbf{U_C}\, diag(1 \;\; 1 \;\; \det(\mathbf{U_C})) \qquad \mathbf{V}_+ = \mathbf{V_C}\, diag(1 \;\; 1 \;\; \det(\mathbf{V_C})) \tag{3.26}$$

The optimal attitude solution is then given by

$$\mathbf{A} = \mathbf{U}_+ \mathbf{V}_+^T \tag{3.27}$$

The singular value decomposition in equation (3.22) transforms the baseline configuration to an equivalent orthonormal basis. At least three noncoplanar baselines must exist to perform this transformation, i.e. $\mathbf{B}$ must be full rank.

If this is not true a solution can still be found as long as three noncoplanar line-of-sight vectors exist. In such a case it is necessary to perform an SVD of $\mathbf{S}$ and then choosing $\mathbf{W}_S$ as in equation (3.23).

Since the line-of-sight vectors change in time, an SVD must be performed at each sample time, which greatly increases the computational burden.

In both cases, the value of the other weight matrix also has to be chosen after some tuning criteria.

3.5 New Algorithm

This method is due to [Crassidis and Markley, 1997] and converts the phase measurements into vector measurements by minimizing the following cost function with respect to $\mathbf{s}_j^B$

$$J_j(\mathbf{s}_j^B) = \sum_{i=1}^{m} \sigma_{ij}^{-2} (\Delta r_{ij} - \mathbf{b}_i^T \mathbf{s}_j^B)^2 \quad \text{for} \quad j = 1, 2, ..., n \tag{3.28}$$

where $\mathbf{s}_j^B$ is the jth line-of-sight vector in the body frame. This results in the following expression for $\mathbf{s}_j^B$

$$\mathbf{s}_j^B = \left(\sum_{i=1}^{m} \sigma_{ij}^{-2} \mathbf{b}_i \mathbf{b}_i^T \right)^{-1} \sum_{i=1}^{m} \sigma_{ij}^{-2} \Delta r_{ij} \mathbf{b}_i \quad \text{for} \quad j = 1, 2, ..., n \tag{3.29}$$

It can be seen from (3.29) that at least three non-coplanar baselines must exist in order for the inverse matrix to exist. Again, a solution can still be obtained if only three non-coplanar line-of-sight vectors exist. If this is the case then instead the baselines have to be determined in the reference frame.
Thus, the following expression for $\mathbf{b}_i^R$

$$\mathbf{b}_i^R = \left(\sum_{j=1}^{n} \sigma_{ij}^{-2} \mathbf{s}_j \mathbf{s}_j^T \right)^{-1} \sum_{j=1}^{n} \sigma_{ij}^{-2} \Delta r_{ij} \mathbf{s}_j \quad \text{for} \quad i = 1, 2, ..., m \tag{3.30}$$

Analogous to Cohen's algorithm, the computational burden increases drastically for coplanar baselines. This due to the matrix inversion of equation (3.30) which has to be performed at each

sample time, whereas for (3.29) the inverse must be computed only once (provided the noise variances σ_{ij}^2 are constant).

Once the phase measurements have been converted into vector measurements the optimal attitude can be obtained by use of the SVD method.

$$\mathbf{C} = \sum_{j=1}^{n} w_j \, \mathbf{s}_j^B (\mathbf{s}_j^R)^T = \mathbf{U}_C \mathbf{\Sigma}_C \mathbf{V}_C^T \tag{3.31}$$

where the optimal attitude $\mathbf{A}$ is given by equations (3.26-3.27).
A proper weight can be obtained from the error covariance of $\mathbf{s}_j^B$ [Crassidis and Markley, 1997]

$$w_j = \frac{1}{3} tr\big(\mathbf{P}_j^{-1}\big) = \frac{1}{3} tr\bigg(\sum_{i=1}^{m} \sigma_{ij}^{-2} \mathbf{b}_i \mathbf{b}_i^T\bigg) \tag{3.32}$$

3.6 ALLEGRO

The ALLEGRO (*Attitude Lean-Loping-Estimator using GPS Recursive Operations*) algorithm uses a one time-step ahead approach to propagate a simple kinematics model for attitude determination [Crassidis et al., 1999a].
It is assumed that the non-linear model of the state and output estimates can be described by

$$\dot{\mathbf{x}}(t) = \mathbf{f}[\,\mathbf{x}(t), t\,] + \mathbf{G}(t)\mathbf{d}(t) \tag{3.33}$$
$$\mathbf{z}(t) = \mathbf{h}[\,\mathbf{x}(t), t\,] \tag{3.34}$$

where $\mathbf{G}$ is the model-error distribution matrix and $\mathbf{d}$ is the model error vector which has to be determined.
The algorithm does not require a dynamics model, it assumes that the attitude is adequately modeled by the constamt model error $\mathbf{d}$ between measurements.
The model equations are described by

$$\dot{\boldsymbol{q}} = \frac{1}{2} \bar{\mathbf{d}} \otimes \boldsymbol{q} \tag{3.35}$$
$$\Delta r_{ij} = \mathbf{b}_i^T \mathbf{A}(\boldsymbol{q}) \mathbf{s}_j \tag{3.36}$$

where $\bar{\mathbf{d}}$ is the fourth dimensional equivalent of $\mathbf{d}$ understood in the sense $\bar{\mathbf{d}} = [\,\mathbf{d}^T \; 0\,]^T$
The optimal value for $\mathbf{d}$ is obtained by minimizing a loss function consisting of the weighted sum square of the measurements-minus-estimate residuals plus the weighted sum square of the model correction (see [Crassidis et al., 1999a] for details).
The result is the following expression for $\mathbf{d}$

$$\mathbf{d} = -\frac{1}{\Delta t} \Bigg\{ \sum_{i=1}^{m} \sum_{j=1}^{n} \sigma_{ij}^{-2} [\mathbf{A}\mathbf{s}_j]^{\times} \mathbf{b}_i \mathbf{b}_i^T ([\mathbf{A}\mathbf{s}_j]^{\times})^T \Bigg\}^{-1} \times \sum_{i=1}^{m} \sum_{j=1}^{n} \sigma_{ij}^{-2} [\mathbf{A}\mathbf{s}_j]^{\times} \mathbf{b}_i (\Delta r_{ij} - \mathbf{b}_i^T \mathbf{A}\mathbf{s}_j) \tag{3.37}$$

where Δt is the sampling period between measurements.
Once the model correction has been calculated the new state vector is obtained by discrete propagation of the old estimate

$$\boldsymbol{q} = (\alpha \mathbf{1}_{4\times 4} + \gamma \, [\bar{\boldsymbol{\rho}}^{\otimes}] \,) \, \boldsymbol{q}' \tag{3.38}$$

where

$$\alpha = \cos\left(\frac{1}{2}\|\mathbf{d}\|\Delta t\right) \tag{3.39}$$

$$\gamma = \sin\left(\frac{1}{2}\|\mathbf{d}\|\Delta t\right) \tag{3.40}$$

$$\boldsymbol{\rho} = \mathbf{d}/\|\mathbf{d}\| \tag{3.41}$$

The ALLEGRO algorithm is robust with respect to initial condition errors. If the initial condition is in the correct hemisphere the solution is guaranteed to converge provided there is at least two baselines and two line-of-sight vectors.
Though, if the algorithm is not initiated in the correct hemisphere a sign ambiguity will arise.

3.7 Bar-Itzhack

Conversion from phase measurements to vector measurements can be done in a more straightforward manner using only two non-collinear baselines [Bar-Itzhack et al., 1998].
If the baselines form the first two axes of a Cartesian triad then the line-of-sight vectors in the body frame can be directly formed from the differential phase measurements

$$\mathbf{s}_j^B = \begin{bmatrix} \Delta\bar{r}_{1j} \\ \Delta\bar{r}_{2j} \\ \sqrt{1-(\Delta\bar{r}_{1j})^2-(\Delta\bar{r}_{2j})^2} \end{bmatrix} \tag{3.42}$$

where the bar symbol indicates a normalized value understood in the sense

$$\Delta\bar{r}_{ij} = \frac{\Delta r_{ij}}{\|\mathbf{b}_i\|} \qquad \text{and} \qquad \bar{\mathbf{b}}_i = \frac{\mathbf{b}_i}{\|\mathbf{b}_i\|} \tag{3.43}$$

It should be noted that the third component of $\mathbf{s}_j^B$ is chosen as the positive root of the expression. This corresponds to the fact that only signals from GPS satellites above the antenna plan, and thus in the positive direction of the third axis, are received by the antennas.
With the line-of-sight vectors calculated in the body frame the problem of estimating the attitude is now in the form of Wahba and can be solved using vector based methods like QUEST, FOAM or Singular Value Decomposition as described in section 3.4

This algorithm is very simple and requires a minimum of computations to convert the measurements into vector form. In present form the baselines have to define Cartesian axes but this is easily extended to the general case of any non-collinear baselines as shown in [Bar-Itzhack et al., 1998].

3.8 Bar-Itzhack 2

[Bar-Itzhack et al., 1998] also present a gradient projection technique for finding the optimal attitude using phase measurements. The algorithm is based on the quaternion representation

and requires only two baselines.
The general GPS cost function in equation 3.4 can be expressed in quaternion form for two baselines as

$$J(\boldsymbol{q}) = \frac{1}{4}\boldsymbol{q}^T\Big[\sum_{i=1}^{2}\sum_{j=1}^{n}\mathbf{M}(i,j)\boldsymbol{q}\boldsymbol{q}^T\mathbf{M}(i,j)\Big]\boldsymbol{q} \tag{3.44}$$

where

$$\mathbf{M}(i,j) = w_{ij}\big((\Delta\bar{r}_{ij})\mathbf{1}_{4\times 4} - \mathbf{L}(i,j)\big) \tag{3.45}$$

and

$$\mathbf{L}(i,j) = \begin{bmatrix} \bar{\mathbf{b}}_i\mathbf{s}_j^T + \mathbf{s}_j\bar{\mathbf{b}}_i^T - (\bar{\mathbf{b}}_i^T\mathbf{s}_j)\mathbf{1}_{3\times 3} & \bar{\mathbf{b}}_i \times \mathbf{s}_j \\ (\bar{\mathbf{b}}_i \times \mathbf{s}_j)^T & \bar{\mathbf{b}}_i^T\mathbf{s}_j \end{bmatrix} \tag{3.46}$$

The solution to finding the optimal $\boldsymbol{q}$ is based on an iterative gradient descent method where the $k+1$st iteration is performed as follows:

$$\boldsymbol{q}_{k+1} = \boldsymbol{q}_k + \epsilon\mathbf{h} \tag{3.47}$$

where $\mathbf{h}$ is a four dimensional unit vector which defines the direction of movement from $\boldsymbol{q}_k$ to $\boldsymbol{q}_{k+1}$, and ϵ is the distance to move in that direction. A suitable step size must be found empirically.
The direction of steepest descent, $\mathbf{h}$, is obtained by substituting equation (3.47) into (3.44) and minimizing the resulting expression $J(\epsilon, \mathbf{h})$ with respect to $\mathbf{h}$.
When minimzing $J(\epsilon, \mathbf{h})$ it must be ensured that $\boldsymbol{q}$ and $\mathbf{h}$ maintains unit length, i.e. the following constraints must be satisfied $\boldsymbol{q}^T\boldsymbol{q} = \mathbf{h}^T\mathbf{h} = 1$.
The minimization yields the following expression for $\mathbf{h}$ (see [Bar-Itzhack et al., 1998] for details)

$$\mathbf{h} = -\frac{1}{2|\lambda|}[\mathbf{C}_k - 4J(\boldsymbol{q})\mathbf{1}_{4\times 4}]\boldsymbol{q}_k \tag{3.48}$$

where

$$\lambda = \sqrt{\frac{1}{4}(\mathbf{C}_k\boldsymbol{q}_k)^T(\mathbf{C}_k\boldsymbol{q}_k) - 4J(\boldsymbol{q}_k)^2} \tag{3.49}$$

and $\mathbf{C}_k$ is the center part in the expression of the cost function

$$\mathbf{C}_k = \sum_{i=1}^{2}\sum_{j=1}^{n}\mathbf{M}(i,j)\boldsymbol{q}_k\boldsymbol{q}_k^T\mathbf{M}(i,j) \tag{3.50}$$

If $\|\boldsymbol{q}_{k+1} - \boldsymbol{q}_k\| < \delta q$, where δq is a predetermined constant, the iteration stops. Otherwise k is increased by one and the iterations continues.

Due to the iterative nature of this method the solution obtained is computationally inefficient and the algorithm requires the constants ϵ and δq to be chosen empirically.

3.9 Euler-q

The Euler-q method ([Mortari, 1998]) is a vector based algorithm that uses a new cost function for optimal attitude definition .

The optimality criterion is derived from the Euler axis/angle representation, where $\mathbf{e}$ is a unit vector parallel to the rotation axis and Φ is the rotation angle about this axis.
Since $\mathbf{e}$ is the rotation axis it must remain constant in both coordinate frames and for all vector pairs:

$$\mathbf{e}^T\mathbf{s}_j^R = \mathbf{e}^T\mathbf{s}_j^B \Rightarrow \mathbf{e}^T(\mathbf{s}_j^R - \mathbf{s}_j^B) = (\mathbf{s}_j^R - \mathbf{s}_j^B)^T\mathbf{e} = 0 \tag{3.51}$$

This is the ideal case where no noise is present.

When using the GPS sensor the line-of-sight vectors $\mathbf{s}_j^R$ are obtained from the phase measurements containing additive noise. In this case equation (3.51) does not hold anymore, instead a small angular error d_j is introduced

$$d_j = \mathbf{e}^T\delta\mathbf{s}_j = \delta\mathbf{s}_j^T\mathbf{e} \tag{3.52}$$

where $\delta\mathbf{s}_j$ is a unit vector given by $\delta\mathbf{s}_j = (\mathbf{s}_j^R - \mathbf{s}_j^B)/\|\mathbf{s}_j^R - \mathbf{s}_j^B\|$.

The cost function which has to be minimized can now be defined as

$$J(\mathbf{e}) = \sum_{j=1}^{n} w_j^* d_j^2 = \sum_{j=1}^{n} w_j^* \mathbf{e}^T\delta\mathbf{s}_j\delta\mathbf{s}_j^T\mathbf{e} = \mathbf{e}^T\mathbf{H}\mathbf{e} \tag{3.53}$$

where the symmetric matrix $\mathbf{H}$ is given by

$$\mathbf{H} = \sum_{j=1}^{n} w_j^*\delta\mathbf{s}_j\delta\mathbf{s}_j^T \tag{3.54}$$

The relative weights w_j^* depend on the sensor errors ξ_j expressed as the angle to the true direction of $\mathbf{s}_j^R$. If this pointing error is small then $\delta\mathbf{s}_j$ and $\mathbf{e}$ becomes nearly perpendicular ($d_j \approx 0$) and the sample should be weighted heavier.
The worst case for the deviation of $\delta\mathbf{s}_j$ from the perpendicular case is given by the ξ_j^* angle which depend upon the sensor error ξ_j and the angle θ between $\mathbf{s}_j^R$ and $\mathbf{s}_j^B$. As can be seen from the spherical triangle in figure 3.3, the maximum deviation of $\delta\mathbf{s}_j$ is obtained from

$$\sin\theta_j \sin\xi_j^* = \sin\xi_j \tag{3.55}$$

Hence, the expression for the relative weights w_j^* becomes

$$w_j^* = \frac{1}{\xi_j^* \sum_{k=1}^{n}(1/\xi_k^*)} \tag{3.56}$$

Minimizing equation 3.53 with respect to $\mathbf{e}$, and including the constraint that $\mathbf{e}$ must be a unit vector, we get

$$J'(\mathbf{e}) = \mathbf{e}^T\mathbf{H}\mathbf{e} - \lambda(\mathbf{e}^T\mathbf{e} - 1) \tag{3.57}$$

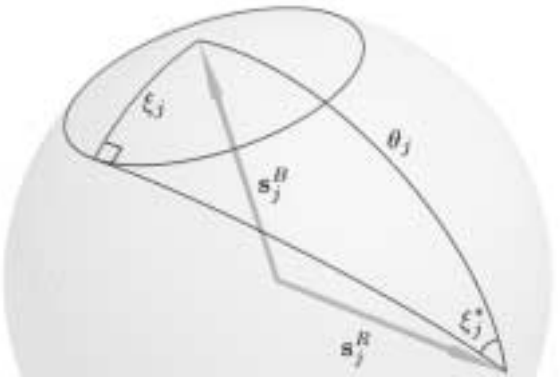

Figure 3.3: Error in the $\delta \mathbf{s}_j$ direction [Mortari, 1998].

A necessary condition for stationarity is

$$\frac{dJ'(\mathbf{e})}{d\mathbf{e}} = 2\mathbf{H}\mathbf{e} - 2\lambda\mathbf{e} = 0 \Rightarrow \mathbf{H}\mathbf{e} = \lambda\mathbf{e} \tag{3.58}$$

Which implies that the searched Euler axis is the eigenvector of $\mathbf{H}$ associated with the λ eigenvalue. In order for $J(\mathbf{e})$ to be a minimum, λ has to be the smallest of the eigenvalues.
The Euler axis can be obtained by performing an eigenanalysis of $\mathbf{H}$, but because $\mathbf{H}$ is symmetric the eigenvalues can be computed using faster methods as described in [Mortari, 1998].

Once the Euler axis has been obtained the Euler angle Φ can be found from the following conditions [Mortari, 1998]

$$\sin\Phi = (1/D)\mathbf{z}^T\mathbf{e} \tag{3.59}$$
$$\cos\Phi = (1/D)(tr[\mathbf{C}] - \mathbf{e}^T\mathbf{C}\mathbf{e}) \tag{3.60}$$

where

$$D^2 = (\mathbf{z}^T\mathbf{e})^2 + (tr[\mathbf{C}] - \mathbf{e}^T\mathbf{C}\mathbf{e})^2 \quad \text{and} \quad \mathbf{z} = \sum_{j=1}^{n} w_j \mathbf{s}_j^B \times \mathbf{s}_j^R \tag{3.61}$$

and the matrix $\mathbf{C}$ is defined as in equation 3.31.

The method of using differential vector measurements $\delta\mathbf{s}_j$ fails in the case of $\Phi \to 0$, which implies that first $\mathbf{A} \to \mathbf{1}$, then $\mathbf{s}_j^R \to \mathbf{s}_j^B$, then $(\mathbf{s}_j^R - \mathbf{s}_j^B) \to \mathbf{0}$, and finally $\mathbf{H} \to \mathbf{0}$.
It may also be shown that the eigenanalysis of $\mathbf{H}$ fails in the case where the Euler axis and all the observed vectors are co-planar.
To avoid these two types of singularities [Mortari, 1998] applies the *method of sequential rotations* (MSR). MSR states that if the n unit vector pairs $(\mathbf{s}_j^B, \mathbf{s}_j^R)$ imply the optimal attitude matrix $\mathbf{A}$ then the n unit vector pairs $(\mathbf{s}_j^B, \mathbf{s}_j^*)$ where $\mathbf{s}_j^* = \mathbf{R}\mathbf{s}_j^R$ and $\mathbf{R}$ is an arbitrary rotation matrix, imply the optimal attitude matrix $\mathbf{F}$, related to $\mathbf{A}$, as $\mathbf{F} = \mathbf{A}\mathbf{R}^T$.
Now, if the set of unit vectors $(\mathbf{s}_j^R, \mathbf{s}_j^B)$ imply a singularity then another set $(\mathbf{s}_j^R, \mathbf{s}_j^*)$ in general would not imply a singularity too. Hence the MSR computes the optimal attitude matrix $\mathbf{F}$ using

the rotated vector set $\mathbf{s}_j^*$.
To minimize the number of extra calculations needed to obtain $\mathbf{s}_j^*$ (and eventually $\mathbf{A}$) $\mathbf{R}$ should be chosen as one of the three matrices that rotate about one of the coordinate axes by a π angle.

$$\mathbf{R}_1 = \begin{bmatrix} 1 & 0 & 0 \\ 0 & -1 & 0 \\ 0 & 0 & -1 \end{bmatrix} \quad \mathbf{R}_2 = \begin{bmatrix} 1 & 0 & 0 \\ 0 & 1 & 0 \\ 0 & 0 & -1 \end{bmatrix} \quad \mathbf{R}_3 = \begin{bmatrix} -1 & 0 & 0 \\ 0 & -1 & 0 \\ 0 & 0 & 1 \end{bmatrix} \tag{3.62}$$

Using these matrices the data set $\mathbf{s}_j^*$ can be obtained from $\mathbf{s}_j^B$ by simply changing the sign of two rows and $\mathbf{A}$ can be found from $\mathbf{F}$ by changing the sign of two columns.
Also, the new data matrix $\mathbf{B}$ can be obtained from the old by a change in signs.

An occurring singularity can be detected in the eigen values of $\mathbf{H}$. The condition $\lambda_2 - \lambda_1 > \zeta$, where ζ is a small positive tolerance factor which has to be determined empirically, indicates that an optimal Euler axis is sufficiently identifiable from the data set.
If on the other hand $\lambda_2 - \lambda_1 < \zeta$ then the MSR is invoked about another axis until $\lambda_2 - \lambda_1 > \zeta$. If $\lambda_2 - \lambda_1 < \zeta$ for all three axes then an unsolvable singularity has occurred (i.e. all line-of-sight vectors are parallel) and attitude determination is aborted.

3.10 Geometric descent

The geometric descent algorithm ([Park et al., 1999]) uses the method of steepest descent which is generalized to SO(3) by taking advantage of its Lie group structure. The problem then becomes one of unconstrained minimization.

The method is iterative with the attitude matrix of the $k+1$ iteration given by

$$\mathbf{A}_{k+1} = \mathbf{A}_k e^{\mathbf{\Omega}_k t_k} \tag{3.63}$$

and

$$t_k = \arg\min_{t \in \mathcal{R}} J(\mathbf{A}_k e^{\mathbf{\Omega}_k t}) \tag{3.64}$$

The direction of rotation is given by a skew symmetric matrix of the normalized angular rate vector, $\mathbf{\Omega} = [\bar{\boldsymbol{\omega}}^\times]$. And the size of the rotation is given by the scalar t_k.

The cost function is similar to the one used by Cohen in section 3.4 and can be expressed as

$$\begin{aligned} J(\mathbf{A}) &= \left\| \Delta\mathbf{R} - \mathbf{B}^T\mathbf{A}\mathbf{S} \right\|^2 \\ &= tr\big((\Delta\mathbf{R} - \mathbf{B}^T\mathbf{A}\mathbf{S})(\Delta\mathbf{R} - \mathbf{B}^T\mathbf{A}\mathbf{S})^T\big) \\ &= tr\big(\mathbf{A}\mathbf{N}\mathbf{A}^T\mathbf{Q} - 2\mathbf{A}\mathbf{W}\big) + tr\big(\Delta\mathbf{R}(\Delta\mathbf{R})^T\big) \end{aligned} \tag{3.65}$$

where $\mathbf{N} = \mathbf{S}\mathbf{S}^T$, $\mathbf{Q} = \mathbf{B}\mathbf{B}^T$ and $\mathbf{W} = \mathbf{S}\mathbf{R}^T\mathbf{B}^T$. Because the last term is independent of $\mathbf{A}$ it can be neglected.
To find the direction of steepest descent we parametrize a neighborhood of $\mathbf{A}_0$ by expanding it as an exponential power series.

$$\mathbf{A}(\mathbf{\Omega}) = \mathbf{A}_0\big(\mathbf{1}_{3\times 3} + \mathbf{\Omega} + \frac{\mathbf{\Omega}^2}{2!} + \dots\big) \tag{3.66}$$

Then to first order in $\mathbf{\Omega}$ and inserting $\mathbf{A}$ into equation (3.65) the following expression is obtained.

$$\begin{aligned} J(\mathbf{A}) &= tr\left(\mathbf{A}_0(\mathbf{1}_{3\times 3}+\mathbf{\Omega})\mathbf{N}(\mathbf{1}_{3\times 3}-\mathbf{\Omega})\mathbf{A}_0^T\mathbf{Q} - 2\mathbf{A}_0(\mathbf{1}_{3\times 3}+\mathbf{\Omega})\mathbf{W}\right) \\ &= tr\left(\mathbf{A}_0\mathbf{N}\mathbf{A}_0^T\mathbf{Q} - 2\mathbf{A}_0\mathbf{W}\right) + tr\left(\mathbf{A}_0\mathbf{\Omega}\mathbf{N}\mathbf{A}_0^T\mathbf{Q} - \mathbf{A}_0\mathbf{N}\mathbf{\Omega}\mathbf{A}_0^T\mathbf{Q}\right. \\ &\quad \left. -2\mathbf{A}_0\mathbf{\Omega}\mathbf{W}\right) + h.o.t. \end{aligned} \tag{3.67}$$

Discarding higher-order terms and taking advantage of the fact that $\mathbf{N}$ and $\mathbf{Q}$ are symmetric, equation 3.67 can be expressed as a linear function of $\mathbf{\Omega}$.
The gradient of the cost function at $\mathbf{A}$ is therefore given by

$$\nabla J(\mathbf{A}) = \mathbf{\Omega} = (\mathbf{N}\mathbf{A}_0^T\mathbf{Q}\mathbf{A}_0 - \mathbf{W}\mathbf{A}_0) - (\mathbf{N}\mathbf{A}_0^T\mathbf{Q}\mathbf{A}_0 - \mathbf{W}\mathbf{A}_0)^T \tag{3.68}$$

Once the direction has been determined the size of the rotation is obtained by minimizing the cost function of the propagated attitude with respect to t_k

$$\min_{t\in\mathcal{R}} J(t) = tr\left(\mathbf{A}e^{\mathbf{\Omega}t}\mathbf{N}e^{-\mathbf{\Omega}t}\mathbf{A}^T\mathbf{Q} - 2\mathbf{A}e^{\mathbf{\Omega}t}\mathbf{W}\right) \tag{3.69}$$

Recalling that $e^{\mathbf{\Omega}t} = \mathbf{1}_{3\times 3} + \mathbf{\Omega}\sin t + \mathbf{\Omega}^2(1-\cos t)$ the cost function can be expressed as a periodic harmonic function with period 2π.

$$J(t) = c_1\sin t + c_2\cos t + c_3\sin 2t + c_4\cos 2t + c_5 \tag{3.70}$$

where the coefficients are defined as $c_1 = a + c$, $c_2 = -b - 2e$, $c_3 = -\frac{c}{2}$, $c_4 = -\frac{d}{2} + \frac{e}{2}$ and $c_5 = b + \frac{d}{2} + \frac{3e}{2} + f$, where

$$\begin{aligned} a &= tr\left((\mathbf{\Omega}\mathbf{N} - \mathbf{N}\mathbf{\Omega})\mathbf{A}^T\mathbf{Q}\mathbf{A} - 2\mathbf{\Omega}\mathbf{W}\mathbf{A}\right) \\ b &= tr\left((\mathbf{N}\mathbf{\Omega}^2 + \mathbf{\Omega}^2\mathbf{N})\mathbf{A}^T\mathbf{Q}\mathbf{A} - 2\mathbf{\Omega}^2\mathbf{W}\mathbf{A}\right) \\ c &= tr\left((\mathbf{\Omega}\mathbf{N}\mathbf{\Omega}^2 - \mathbf{\Omega}^2\mathbf{N}\mathbf{\Omega})\mathbf{A}^T\mathbf{Q}\mathbf{A}\right) \\ d &= -tr\left(\mathbf{\Omega}\mathbf{N}\mathbf{\Omega}\mathbf{A}^T\mathbf{Q}\mathbf{A}\right) \\ e &= tr\left(\mathbf{\Omega}^2\mathbf{N}\mathbf{\Omega}^2\mathbf{A}^T\mathbf{Q}\mathbf{A}\right) \\ f &= tr\left(\mathbf{N}\mathbf{A}^T\mathbf{Q}\mathbf{A} - 2\mathbf{W}\mathbf{A}\right) \end{aligned} \tag{3.71}$$

A minimum exist where the derivative of $J(t)$ with respect to t is zero, hence

$$c_1\cos t - c_2\sin t + 2c_3\cos 2t - 2c_4\sin 2t = 0 \tag{3.72}$$

Making the trigonometric half-angle substitution $x = \tan\frac{t}{2}$, so that $\sin t = \frac{2x}{1+x^2}$, $\cos t = \frac{1-x^2}{1+x^2}$, $\sin 2t = \frac{4x(1-x^2)}{(1+x^2)^2}$, and $\cos 2t = \frac{x^4-6x+1}{(1+x^2)^2}$.

$$(2c_3 - c_1)x^4 - 2(c_2 - 4c_4)x^3 - 12c_3x^2 - 2(c_2 + 4c_4)x + (c_1 + 2c_3) = 0 \tag{3.73}$$

The roots are obtained using standard mathematical tools.

3.11 Comparison

Algorithm	**Strength**	**Weakness**
Kalman filter	• Highly accurate	• High computational burden • Numerically unstable • Needs tuning
Single point	• Easy to implement	• Not very robust
Cohen's method		• Computationally expensive if baselines are coplanar • Tuning of weight matrix
New algorithm		• Computationally expensive if baselines are coplanar
Allegro	• Always converges provided there is at least two baselines and two line-of-sight vectors • Low computational burden • Easy to implement	
Itzhack	• Extremely fast and simple	• Highly sensitive towards bad measurements
Itzhack-2		• Iterative • High computational burden
Euler-q	• Fast	• Singularities are often encountered and requires extra computations to avoid • Weight matrices are laborious to compute
Geometric descent		• Iterative • High computational burden

Table 3.2: Comparison of algorithms

4 Simulation results

When evaluating the performance of different algorithms a large set of parameters can be used for comparison. Obviously, the precision that can be obtained using the particular algorithm is an important factor, but also, the number of computations needed to obtain that accuracy must be considered.

Recursive algorithms that use an á priori estimate of the attitude are often sensitive to the accuracy of the initial estimate and thus the ability to converge to the correct attitude solution becomes important.

In subsequent sections the following performance parameters will be evaluated based on simulated data

- Accuracy
- Computational efficency
- Ability to converge from erroneous attitude estimates

This is by no means an exhaustive list of performance parameters and further criterias could arguably be added. However, given that high-precision is the object of intererst, the investigation has been limited to the above mentioned indexes.

4.1 Accuracy

To test the accuracy of the algorithms differential phase measurements and line-of-sight vectors were generated in a simulation program for a various number of GPS satellites and baseline configurations.
The simulation time was set to 5 min. during which the baseline configuration was rotated 360 deg. around the w-axis. The sample time was fixed at 1 sec. and the white noise was added to the simulated phase measurements. Earlier field tests had revealed a noise variance of $\sigma_N = 0.028\lambda$ for this kind of receiver [Fossa et al., 1998].
To investigate the influence the baseline configuration has on the accuracy of the algorithms, three different configurations were simulated.

- **3 coplanar** baselines - same configuration as the actual test platform (see section 2.1).
- **2 coplanar** baselines - same as above but without baseline $\mathbf{b}_2$.
- **3 non-coplanar** baselines - same as above but with a third baseline perpendicular to the two others and of same length (orthonormal).

As a measure of the combined estimation error the RMS value of the angular error around each body coordinate axis was calculated and the RSS value was obtained as the norm of this error vector.
For reason of comparison the Bar-Itzhack algorithm, which is only defined for 2 baselines, was modified to also encompass orthonormal configurations in the following way

$$\mathbf{s}_j^B = \frac{[\Delta\bar{r}_{1j} \;\; \Delta\bar{r}_{2j} \;\; \Delta\bar{r}_{3j}]^T}{\sqrt{(\Delta\bar{r}_{1j})^2 + (\Delta\bar{r}_{2j})^2 + (\Delta\bar{r}_{3j})^2}} \tag{4.1}$$

Algorithm	RSS error in degrees		
	2 coplanar	3 coplanar	3 non-coplanar
Kalman filter	0.1756	0.1513	0.1667
Single-point	0.4933	0.3779	0.4387
ALLEGRO	0.4936	0.3682	0.4420
Geometric descent	(Does not converge)		0.4413
New Algorithm + SVD	0.5366	0.4043	0.4334
Bar-Itzhack + SVD	0.5282	(Undefined)	0.4442
Cohen	0.5320	0.4102	0.4434
Euler-q	0.5412	0.4084	0.4423

Table 4.1: Result of accuracy test with three different baseline configurations.

It is clearly seen from the results in table 4.1 that the Kalman filter is the most accurate of the algorithms tested, with an estimation error as little as between one third and half of any other. This could also be expected from an algorithm that propagates a model of the satellite movement and combines this with the measurements in a (sub)optimal way.

Also, in the case of only two baselines, the recursive algorithms that use differential phase measurements directly obtain a slightly better precision over the algorithms that use converted vector measurements. This difference does not exist when the baselines are orthogonal thus indicating that direction in three dimensions is more difficult to estimate with coplanar baselines. This is caused by the way the measurement noise affects the vector components in this case.

The results also show that increasing the number of baselines also increases the accuracy which of course could be expected. Given the same number of baselines, three in this case, a planar configuration proves more accurate than an orthonormal configuration. One might argue that a configuration spanning all three dimensions would have the highest observability of the satellites. However, when the rotational movement is fairly simple, e.g. a constant rotation axis parallel to a body coordinate axis, baselines perpendicular to the rotation axis provide more information about the movement than baselines parallel to it.

4.2 Computational efficiency

To evaluate the computational speed of the algorithms the MATLAB function *flops* was used which indicates the approximate cumulative number of floating point operations. Using this function operations like addition, subtraction, multiplication and division are all counted as one flop each. Elementary functions such as sine, cosine, square root e.t.c. are also counted as one flop.
Figure 4.1 shows the number of flops required at each sample time for a configuration of two baselines and 2 to 6 satellites usable for attitude estimation. In case of the iterative algorithms, the graph indicates the number of flops for each iteration. The algorithms which convert phase measurements into vector measurements have been combined with the SVD method for the sake of easier comparison. For the same reason the Euler-q algorithm was tested with vector estimates provided by the *New Algorithm*.

Again, the Kalman filter separates itself from the other methods. The number of computations

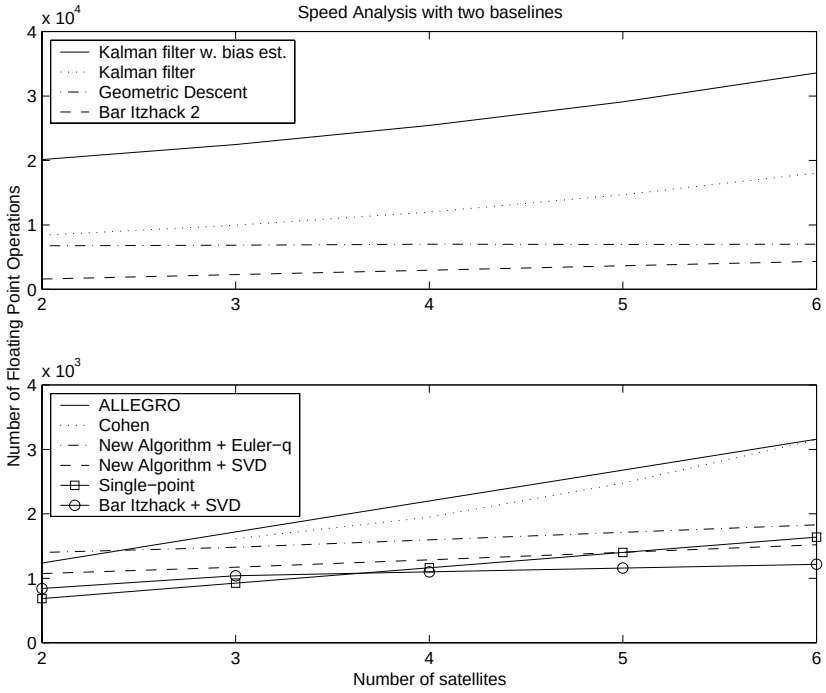

Figure 4.1: Computational efficiency with two baselines. (Top) Slowest algorithms (Bottom) Fastest algorithms. Notice the different scaling of the axes.

required at each sample time is roughly ten times greater than for some of the faster algorithms. When including line bias calibration into the workings of the Kalman filter, this difference increases to a factor of more than twenty! Since however the line bias values remain constant over time the filter would only be needed to run in calibration mode for a short time period following initiation.

The Geometric Descent algorithm is also among the slowest, but unlike any of the other algorithms, the computational burden of this algorithm does not increase with the number of satellites. The reason for this, is that after the 3-by-3 matrices $\mathbf{N}$ and $\mathbf{W}$ have been obtained from the most recent measurements and line-of-sight vectors, the rest of the computations follow directly from these matrices. Most of the required computations are needed to obtain the exact step size t (see equation (3.71)). Thus, using a rough estimate instead of the exact value would probably speed up the algorithm significantly. As this algorithm is iterative, several iterations might be necessary to obtain an acceptabel accuracy, hereby further increasing the computation time. This fact must also be considered when using the other iterative algorithm, *Bar-Itzhack 2*.

The Single-point algorithm is the fastest of the ones tested, for three or less usable GPS satellites. In case of 4 or more satellites the SVD method, applied to vectors estimated by the Bar-Itzhack approach, requires the fewest computations. These two algorithms are some of the most simple, but as it was shown in the accuracy test, should not be discarded for their simplicity.

The vector based algorithm *Euler-q* is also one of the faster. Though, due to the rather comprehensive calculations of the weight factors, it requires an extra 350 flops at each sample time compared to the SVD method. Adding further to the flop count, the built-in MSR method re-

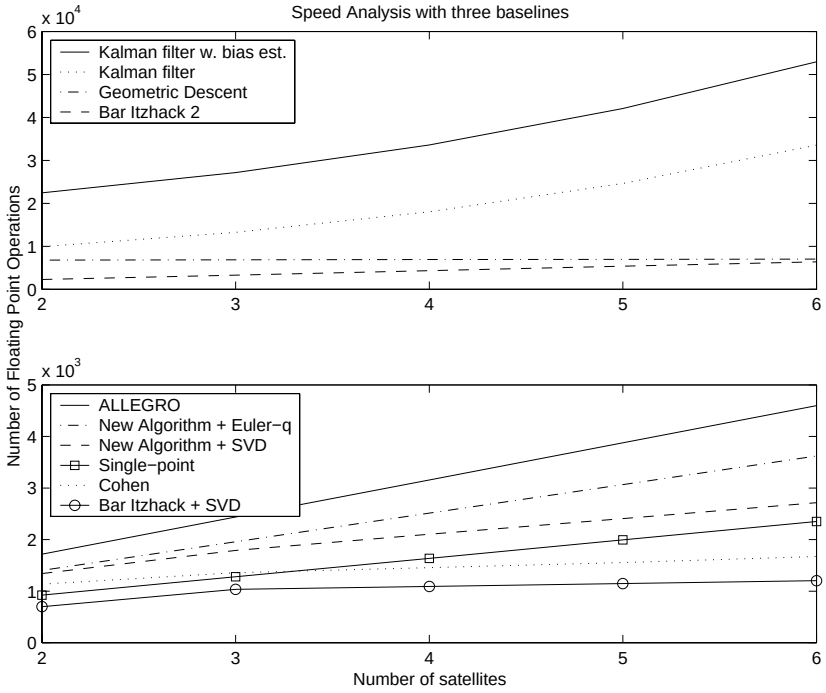

Figure 4.2: Computational efficiency with three baselines. (Top) Slowest algorithms (Bottom) Fastest algorithms.

quires the re-computation of some matrices whenever it is near a singularity.

In between the fast and the slow algorithms we have *ALLEGRO* and *Cohen's method*. Cohen also uses the SVD method to find the optimal $\mathbf{A}$ but since the baseline matrix is not full rank the SVD method has to be invoked twice at each sample time, significantly slowing this algorithm down.

In the case of three orthogonal baselines the relative speed of the algorithms remain unchanged with few exceptions (see figure 4.2). The overall computational burden has only increased slightly for each algorithm but it increases faster for a growing number of sight lines. The fastest algorithm is still the *Bar-Itzhack* combined with the SVD method, but since the baseline matrix is now full rank, Cohen's method becomes faster than almost any of the others. This shows how the choice of algorithm should reflect the baseline configuration.

4.3 Convergence

A Monte Carlo simulation was performed to test the effect an inaccurate initial attitude estimate has on the recursive algorithms. 10000 initial estimates were randomly generated and the time required for the following estimation errors to reach RSS ≤ 0.5 deg. was recorded as the convergence time. Specifically, each component of the initial attitude quaternion was generated from a uniform random distribution in the interval -1 to 1 using the MATLAB function *rand*, following which the quaternion was normalized.

As shown in figure 4.3 neither of the three algorithms has a convergence of 100%. This means that there are certain initial attitudes from which these algorithms does not converge to the

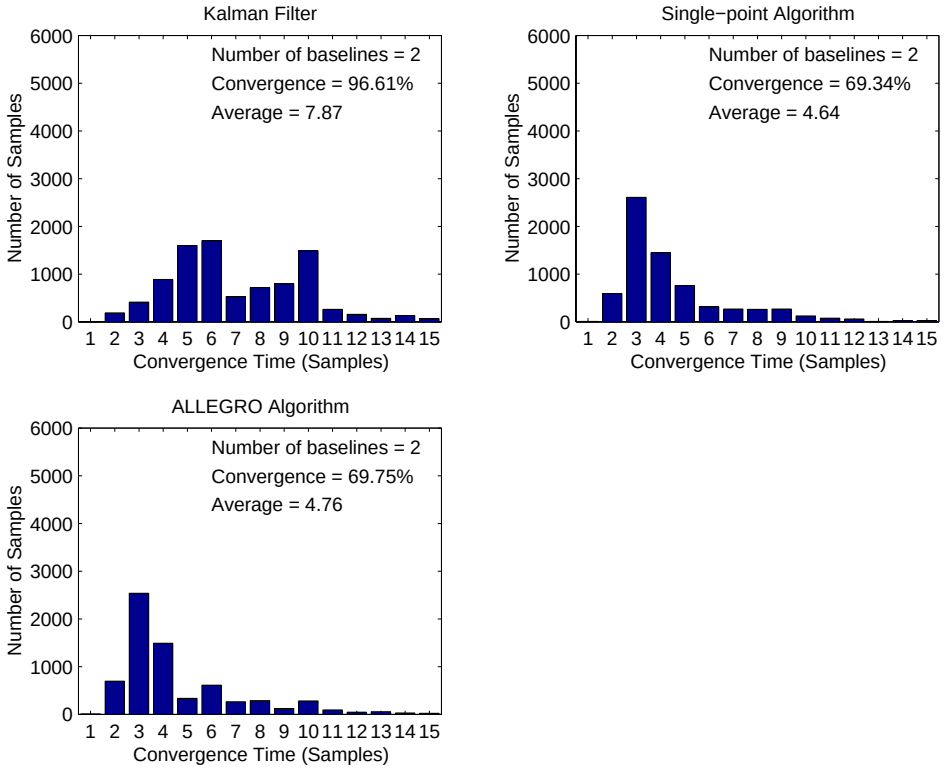

Figure 4.3: Monte Carlo convergence analysis for a configuration of two baselines

correct solution. The Kalman filter has the highest rate of convergence only failing in three percent of the cases. The ALLEGRO and Single-point algorithms performs almost identically, both failing in almost one out of three times.

Considering the initial states, from where the algorithms eventually *do* converge, the average convergence time is about 7.9 for the Kalman filter and 4.7 for the two others. Hence, the Kalman filter is slower but more reliable. A reason for this could be the way that this algorithm calculates the attitude correction as a combination of measurements and model-based predictions. These predictions prevent the filter from making large corrections, effectively slowing down the converging process in accordance with the modeled behavior.

The relative influence of the model prediction is determined by tuning the filter. To speed up the converging process the filter was tuned to downgrade the model influence by setting $\mathbf{Q} = \mathbf{1}$.

Although the Kalman filter does not converge as fast as the other algorithms 95% of the 10000 initial estimates converge within 20 samples, which is a high number considering that convergence is not guaranteed.

In the case of non-coplaner baselines the Geometric Descent algorithm also becomes an option. By increasing the baseline configuration to span all three dimensions, the four testet algorithms all converge to the correct attitude solution for any initial estimate. Which is a major motivation for using non-coplanar baselines.

Figure 4.4 also shows that the convergence time is reduced by using non-coplanar baselines.

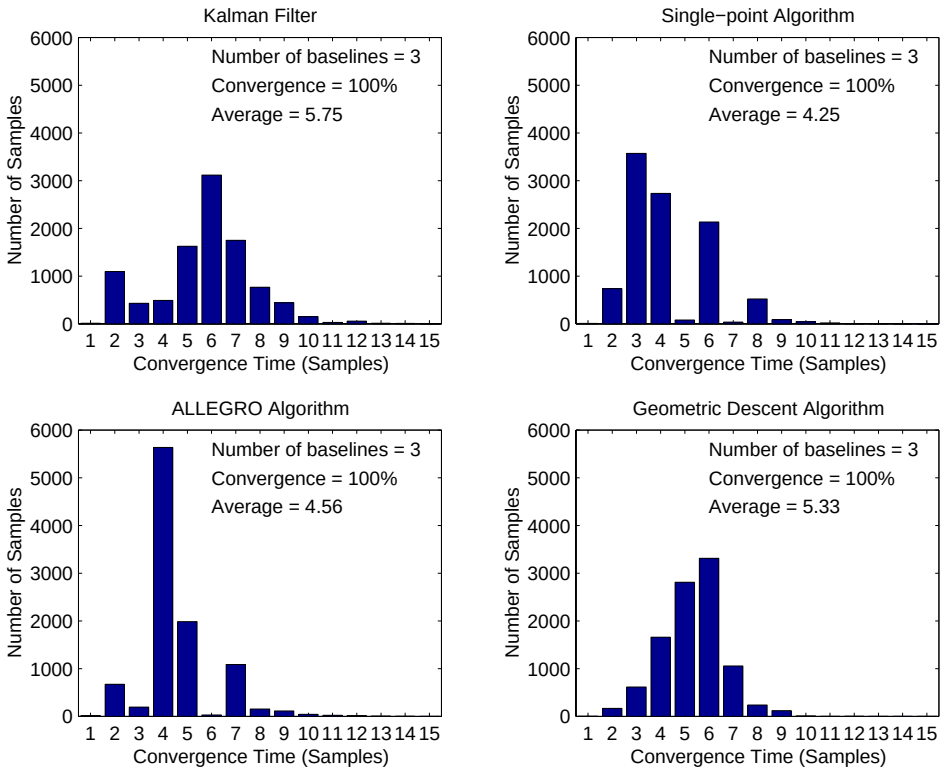

Figure 4.4: Monte Carlo convergence analysis for a configuration of three orthogonal baselines

Still the ALLEGRO and Single-point algorithms prove to be fastest with the Geometric Descent algorithm performing only slightly better than the Kalman filter.

5 Conclusions

High precision satellite missions require attitude determination better than 0.1 deg RMS. To test if this accuracy can be obtained using GPS signal phase interferometry, several different algorithms were implemented and tested on simulated data.

The Kalman filter proved to be the most accurate of the algorithms, actually meeting the 0.1 deg (1σ) requirement for a three baseline configuration. The rest of the algorithms obtained virtually the same accuracy of 0.25 deg (1σ) with the ALLEGRO and Single-point algorithm doing slightly better than the others for a two baseline configuration.
Flop counts showed however, that the superior accuracy of the Kalman filter comes with the price of a computational burden 10 to 20 times higher than most of the other algorithms. Furthermore, Monte Carlo analysis of the recursive algorithms showed that the Kalman filter would converge to the correct attitude solution in 97% of the cases when using coplanar baselines, whereas the ALLEGRO and Single-point only succeeds in 70%. For non-coplanar baselines all the recursive algorithms had 100% convergence rate.

In summary, the Kalman filter seems to be the best choice for high precision missions being the only algorithm of those tested which achieved the accuracy requirement.

By setting the model noise intensity very small, angular errors better than 0.05 deg RMS could be achieved. This however requires very precise knowledge of the inertial moments of the satellite, something which is rarely available on real missions.

The number of computations required per sample could be reduced by avoiding multiplications of entire matrices when off diagonal elements are (close to) zero. Further the matrix inversion involved in calculation of the Kalman gain could be obtained by using pseudo inversion techniques significantly lowering the number of required computations.

5.1 Perspective

The algorithms presented here were tested on simulated data from a baseline configuration similar to the AAU testbed. In addition, configurations of two and three orthogonal baselines were also tested for comparison reasons. The simulated noise was of same magnitude and character as obtained from the Trimble GPS reciever. Thus, the accuracy and convergence results can in principle be applied to missions of same baseline configuration and dynamics.

The result of the speed analysis cannot directly be related to actual spacecraft hardware as the number of computations for the algorithms by no means were minimised. Still, the relative speed of the algorithms must be expected only to change little when implemented in the spacecraft hardware.

5.2 Future Work

Due to alignment problems arising from the limitations of the current mechanical hardware it would be a fruitless effort to implement the algorithms on real data from the testbed. The alignment problem could be solved by upgrading the testbed with a star tracker. This possible solution is under investigation at the present time. Det Obelske Familiefond has provided funding for integration of a star tracker with the AAU testbed. Through a cooperation with Terma Elektronik A/S a star tracker has been made available and the augmentation of the testbed with the star tracker is currently on the way.

Furthermore, the results showed that the baseline configuration had a profound impact on the accuracy, speed and convergence rate of the algorithms. Hence, further efforts should be made to investigate a possibly optimal and mechanically feasible configuration.

6 Alignment

The problem of creating an absolute attitude reference frame when taking outdoor measurements can be approached in several different ways.
The precision of which the absolute reference frame is aligned to the ENU reference frame (see section 2.3) should be as good as possible. As a rule of thumb the alignment should be at least ten times better than the precision aimed for in the experiment.
When trying to determine the attitude of the antenna array with an RMS error of 0.1° or better, the absolute reference frame has to be aligned with a precision of at least 0.01° or 36 arc seconds.

To obtain this degree of precision, two different approaches has been proposed

- Gravity field measurements + Optical alignment
- Star tracker

6.1 Gravity field measurements

When using gravity field measurements the *Up*-axis of the ENU system is aligned to the negative direction of the gravity vector.
For further alignment of the *North*-axis toward true north it is necessary to use an optical alignment technique where a laser beam is bounced off a cubic crystal fixed on the antenna array. The beam has to be reflected at a right angel and is further restricted to pass over two points lying on the same meridian (hereby defining the direction toward true north). These two points have to be precisely determined using the GPS receiver's own position solution, hereby introducing new uncertainties.
This is in effect a calibration which has to take place before any measurements can be made. The attitude of the antenna array has to be read from the angle values of the encoders.
This introduces another problem of alignment seeing that the encoders measure angels relative to their initial values. It means that these angles must all be zero at startup, or put differently, the rotation axes must be orthogonal.
A possible way to ensure this, is to level out the base as well as the top of the turntables using the previously mentioned techniques. Furthermore, both base and top of the turntables must be aligned towards true north using the laser beam and crystal.
All in all, this is a very complicated procedure which possibly has to be repeated between measurement series.

6.2 Star tracker

Another possible approach is to equip the testbed with a star tracker.
By attaching a star tracker to the antenna array the encoders can be removed from the loop.
The star tracker provides the true attitude at all time and neither the base nor the top of the turntables needs to be aligned.
Although, to maintain the validity of the model for the satellite's movement (described in equation (3.10)) the turntables still need to be aligned to some degree.
A star tracker could consist of a CCD camera along with a frame grabber and an algorithm to calculate the true attitude from the images.
The camera must have sufficient resolution and a high sensitivity to light, possibly through the

	Gravity measurement	**Star tracker**
Additional hardware required	• Laser • Crystal cube • Land measurement tripod	• CCD camera • Frame grabber
Additional software required	*None*	• Software to read and store images from frame grabber • Image algorithms to solve for attitude
Additional mechanical requirements	• Precise positioning of crystal cube • Precise right-angel alignment of turntables	• Precise positioning of CCD camera
Obtainable precision	Around 0.01°	Better than 0.01°

Table 6.1: Comparison of alignment methods

use of extra lenses.
The frame grabber must be able to capture the images at the required rate of 1 Hz, and must be of a type compatible with laptop PCs. The amount of space on the hard drive limits the size and number of the images stored.
As for the attitude solution, many off-the-shelf algorithms exist which will do a satisfactory job.

6.3 Comparison

For the reasons mentioned above it must be concluded that the star tracker is the better choice, mainly because of the error sources this solution eliminates, but also because of the material cost and added complexity gravitational measurements require.
However, existing off-the-shelf algorithms are designed to work on images recorded in the vacuum of space. Using these algorithms on images recorded from a platform on the ground introduces new error sources caused by the attenuation and refraction of light in the atmosphere. The attenuation can be easily modeled as a constant gain factor and would therefore not pose a problem. The diffraction would cause the image to distort, changing the apparent direction to the stars and thus reducing the accuracy.
The amount of distortion depends on the direction to the stars relative to zenith. If this angle is zero the light is not diffracted while the most diffraction appears at the horizon.
The angular error caused by diffraction can be investigated using a formula obtained from experiments [Meeus, 1991]

$$R = \frac{1}{\tan\left(h_0 + \frac{7{,}31}{h_0+4{,}4}\right)} \tag{6.1}$$

where h_0 is the altitude in degrees (90° - zenith) and R is the amount of diffraction in arcminutes. Due to mechanical limitations the maximum zenith angle that can be obtained using the testbed is 15 deg. If the FOV of the star tracker is 24 deg then equation 6.1 predicts a maximum angular error of 30.5 arcsec along the edges of the image.

7 Bibliography

7.1 Reference Documents

[Bak, 1999] Bak, T. (1999). *Spacecraft Attitude Determination - a Magnetometer Approach*. PhD thesis, Aalborg University.

[Bar-Itzhack et al., 1998] Bar-Itzhack, I. Y., Montgomery, P. Y., and Garrick, J. C. (1998). Algorithms for attitude determination using the global positioning system. *Journal of Guidance, Control, and Dynamics*, 21(6):846–852.

[Cohen, 1992] Cohen, C. E. (1992). *Attitude Determination Using GPS*. PhD thesis, Stanford University, Department of Aeronautics and Astronautics.

[Conway et al., 1996] Conway, A., Montgomery, P., Rock, S., Cannon, R., and Parkinson, B. (1996). A new motion-based algorithm for gps attitude integer resolution. *Journal of The Institute of Navigation*, 43(2):179–190.

[Crassidis et al., 1999a] Crassidis, J. L., Lightsey, E. G., and Markley, F. L. (1999a). Efficient and optimal attitude determination using recursive global positioning system signal operations. *Journal of Guidance, Control, and Dynamics*, 22(2):193–201.

[Crassidis and Markley, 1997] Crassidis, J. L. and Markley, F. L. (1997). New algorithm for attitude determination using global positioning system signals. *Journal of Guidance, Control, and Dynamics*, 20(5):891–896.

[Crassidis et al., 1999b] Crassidis, J. L., Markley, F. L., and Lightsey, E. G. (1999b). Global positioning system interger ambiguity resolution without attitude knowledge. *Journal of Guidance, Control, and Dynamics*, 22(2):212–218.

[Fossa et al., 1998] Fossa, F., Høgh-Rasmussen, J., Ingwersen, S., and Jensen, M. (1998). Attitudebestemmelse af satellitter med gps. Student report, Aalborg University.

[Lightsey et al., 94] Lightsey, E. G., Cohen, E. E., Feess, W. A., and Parkinson, B. W. (94). Analysis os spacecraft attitude measurements using onboard gps. *Advances in the Astronautical Sciences*, 86:521–532.

[Meeus, 1991] Meeus, J. (1991). *Astronomical Algorithms*. Willmann-Bell, Inc., first edition.

[Mortari, 1998] Mortari, D. (1998). Euler-q algorithm for attitude determination from vector observations. *Journal of Guidance, Control, and Dynamics*, 21(2):328–334.

[Park et al., 1999] Park, F. C., Kim, J., and Kee, C. (1999). Geometric descent algorithms for attitude determination using gps. In *14th World Congress of IFAC*, pages 557–562, Seoul, Korea.

[Shaki, 1998] Shaki, P. (1998). Station first to use gps for attitude control. Space News.